Journal of Thermal Analysis and Calorimetry (2023) 148:12597–12607
https://doi.org/10.1007/s10973-023-12588-1

An impact of MHD and radiation on flow of Jeffrey fluid with carbon nanotubes over a stretching/shrinking sheet with Navier's slip

T. Anusha[1] · U. S. Mahabaleshwar[1] · Suvanjan Bhattacharyya[2]

Received: 17 February 2023 / Accepted: 16 September 2023 / Published online: 24 October 2023

Abstract
This article focuses on MHD flow and heat transfer of Jeffrey fluid due to a stretching/shrinking surface with carbon nanotubes, considering the effects of thermal radiation, heat source/sink parameters, and Navier's slip. Generally, solids offer higher thermal conductivity than fluids. To offer higher thermal conductivity, a new type of nanofluid is formed by suspending two types of carbon nanotubes (CNTs), i.e. single-wall carbon nanotubes (SWCNTs) and multi-wall carbon nanotubes (MWCNTs), which act as nanoparticles, into the base fluid, water. It is intended to enhance the thermal conductivity and mechanical properties of the base fluid. The structure of the problem is an equation of momentum and temperature, which are then converted into a set of ODEs to imitate the MHD flow of carbon nanotubes. The magnetic parameter, radiation parameter, and Navier slip effect significantly affect the structure of the solution to the problem. Carbon nanotubes act as nanoparticles that enhance the heat performance and mechanical properties more than the base fluid, so they have many applications in electronics and transportation. The velocity and temperature profiles, skin friction coefficient, and Nusselt number are observed and discussed through graphs. The results reveal that for stretching case, velocity profile increases with increasing the magnetic field, while the opposite trend observed in shrinking case. We notice that the SWCNT Nanofluids are better nanofluids than the MWCNT Nanofluids. We study from these final results that the usage of CNTs in most cancerous therapies can be more useful than all sorts of nanoparticles.

Keywords CNTs · MHD · Heat source/sink · Navier slip · Jeffrey fluid · Nusselt number

List of symbols

a, c	Constants
B_0	Applied magnetic field (wm^{-2})
β	Constants
C_f	Skin friction coefficient
C_p	Specific heat ($Kg\ m^{-3}$)
d	Stretching/shrinking sheet parameter
f	Similarity variable for velocity
L_1	Navier's slip
M	Magnetic parameter (–)
N_R	Radiation parameter (–)
q_r	Heat flux (Wm^{-2})
Vc	Mass transpiration parameter
Pr	Prandtl number
Nu_x	Local Nusselt number
T	Temperature field (K)
T_w	Wall temperature
T_∞	Ambient temperature
V_w	Wall mass transfer velocity (ms^{-1})
u,v	Velocities along x- and y- direction (ms^{-1})
x, y	Co-ordinate axes (m)

Greek symbols

α	Thermal diffusivity ($m\ s^{-1}$)
β	Deborah number
μ	Dynamic viscosity of nanofluid ($m^2\ s^{-1}$)
ν	Kinematic viscosity ($m^2\ s^{-1}$)
ρ	Density ($Kg\ m^{-3}$)
σ	Electrical conductivity ($S\ m^{-1}$)
η	Similarity variable
θ	Similarity variable for temperature

✉ Suvanjan Bhattacharyya
suvanjan.bhattacharyya@pilani.bits-pilani.ac.in

T. Anusha
anushatchr123@gmail.com

U. S. Mahabaleshwar
u.s.m@davangereuniversity.ac.in

[1] Department of Mathematics, Shivagangotri, Davangere University, Davangere, India

[2] Department of Mechanical Engineering, Birla Institute of Technology and Science Pilani, Pilani Campus, Vidhya Vihar, Pilani, 333 031, Rajasthan, India

λ Stagnation/strength parameter
Γ_1 , Γ_2 Material parameters of Jeffrey fluid

Subscripts

f Parameter of base fluid
nf Parameter of nanofluid
w Parameter at the wall
∞ Ambient condition

Abbreviations

B.Cs Boundary conditions
CNTs Carbon nanotubes
ODE Ordinary differential equations
PDE Partial differential equations

Introduction

The mixture of nanoparticle in a base fluid is named as nanofluid which works efficiently in cooling the system which is in high temperature range and has many thermal applications. Introduction of the MHD force will affect more on the flow due to development of Lorentz force. Magnetohydrodynamic (MHD) flow plays an important part in the production of petroleum products and processes of metallurgy. It is to note that the final product that is formed is dependent on the rate of cooling followed by these processes. In order to separate the metallic materials from the nonmetallic materials, this field of magnetism is used to refine the molten metals. The carbon nanotubes (CNTs) based nanofluid as a heat transfer system. CNTs are a well-known allotrope of family of fullerene exhibiting long and hollow chemical structure compromising of graphene sheets. In a broader sense, two kinds of CNTs exist viz., single and multi-walled. The thermophysical properties of CNTs are subservient along with graphene sheets getting aligned in a sequential manner within the tube which results in this kind of materials to execute properties of metal or semiconductor. Ebaid and Sharif [1] investigated MHD transfer of heat and flow of CNTs-suspended nanofluids over stretching sheet (linear). The flow of MHD in such a particular case was first explored by Sarpakaya [2] and Mahabaleshwar [3–5]. Tiwari et al. [6] investigated the Marangoni convection MHD flow of CNTs through a porous medium with radiation.

Stretching sheet problems are very applicable in many industrial processes such as electronic cooling process, heat exchange between devices, and cooling of engines. Because of this reason, many researchers show an interest on stretching sheet problems. Crane [7] and Sakiadis [8] are pioneers in the investigation of stretching sheet problems. Hayat et al. [9] examined stagnation point of viscous nanofluid over a nonlinear stretching surface with variable thickness.

Hamad [10] and Fang and Zhang [11] examine the MHD flow due to shrinking sheet and shrinking sheet, respectively. Vinay Kumar et al. [12] have investigated the impact of MHD and mass transpiration on the slip flow. Sneha et al. [13] have examined the stagnation point flow over a Jeffrey fluid flow through a stretching/shrinking sheet. Turkyilmazoglu et al.[14] examined the MHD flow, heat and mass transfer of viscoelastic fluid with slip over the stretching surface and got the multiple solutions. Recently, Reddy et al.[15] examine the numerical analysis of the MHD flow of CNT nanofluid over a nonlinear inclined stretching/shrinking sheet with heat generation and viscous dissipation. Norzawary et al.[16] examined on the stagnation point flow in CNTs with suction/injection impacts over a stretching/shrinking sheet.

Mahabaleshwar et al.[17] made the article on the MHD flow with carbon nanotubes by considering the effect of mass transpiration and radiation on it. Mahabaleshwar et al. [18] investigates the MHD flow and mass transfer due to porous media. Turkyilmazoglu [19] studied on exact solution for flow of Jeffrey fluid. The Novelty of the present research is to examine the MHD flow and heat transfer of Jeffrey fluid due to a stretching/shrinking surface with CNTs considering the effects of thermal radiation and Navier's slip. And the motivation is to add the effects CNTs and slips to previous works of momentum and energy with constant and linear wall temperature. Secondly, to provide an analytic solution of the resulting nonlinear system is novel. Moreover, the influence for various physical features as magnetic parameter, mass transpiration, radiation and Prandtl number parameter are presented on the field of flow and analysed thereafter. Investigate the important physical parameters Nusselt number and skin friction (Fig. 1).

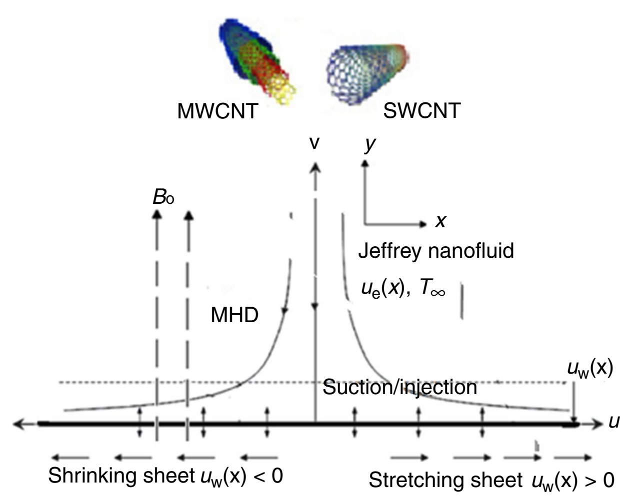

Fig. 1 Schematic diagram of the flow problem

Physical model and explanations

The steady MHD flow and heat transfer of Jeffrey fluid with CNTs due to a stretching/shrinking surface moving with deforming wall velocity $u_w(x)$ is examined and the phenomena of heat transfer with thermal radiation are investigated. The magnetic field of strength B_0 is applied perpendicular to the fluid flow. The fluid flow is along x-axis and y-axis is perpendicular to it. The sheet is stretched/shrinked with the velocity which is proportional to the distance from the origin c. The momentum and temperature governing equations can be modelled as Saif et al. [20], Rao et al. [21], and Maranna et al. [22].

$$\frac{\partial u}{\partial x}+\frac{\partial u}{\partial y}=0, \tag{1}$$

$$\rho_{nf}\left(u\frac{\partial u}{\partial x}+\mathrm{v}\frac{\partial u}{\partial y}\right)=\rho_{nf}u_e\frac{\partial u_e}{\partial x}+\frac{\mu_f}{1+\Gamma_1}\left[\frac{\partial^2 u}{\partial y^2}+\Gamma_2\left(u\frac{\partial^3 u}{\partial x\partial y^2}-\frac{\partial u}{\partial x}\frac{\partial^2 u}{\partial y^2}+\frac{\partial u}{\partial y}\frac{\partial^2 u}{\partial x\partial y}+\mathrm{v}\frac{\partial^3 u}{\partial y^3}\right)\right]-\frac{\sigma_{nf}B_0^2}{\rho_{nf}}(u-u_e) \tag{2}$$

$$u\frac{\partial T}{\partial x}+\mathrm{v}\frac{\partial T}{\partial y}=\frac{\kappa_{nf}}{(\rho c_p)_{nf}}\frac{\partial^2 T}{\partial y^2}-\frac{1}{(\rho c_p)_{nf}}\frac{\partial q_r}{\partial y}, \tag{3}$$

with B.Cs as follows:

$$\begin{array}{llll} u=dcx+A\frac{\partial u}{\partial y}, & v=v_w, & T=T_w(x) & y=0 \\ u\to u_e(x)=ax, & \frac{\partial u}{\partial y}\to 0, & T\to T_\infty & y\to\infty \end{array} \tag{4}$$

here, $u_e(x)=ax$ is the potential flow and wall temperature field $T_w(x)$ is either kept at constant T_w or linearly proportional with x as follows: $T_w(x)=T_w+bx$, $\mathrm{v}_w=-\left(\frac{c\nu_f}{(1+\omega_1)}\right)^{\frac{1}{2}}S$ is wall transpiration, where $\mathrm{v}_w<0$ for suction and $\mathrm{v}_w>0$ for injection. Γ_1 and Γ_2 are material parameters of Jeffrey fluid.

The suitable similarity transformations [19] are as follows:

$$\eta=\left(\frac{c(1+\Gamma_1)}{\nu_f}\right)^{\frac{1}{2}}y,\ u=cx\frac{\partial f}{\partial \eta},\quad \mathrm{v}=-\left(\frac{c\nu_f}{(1+\Gamma_1)}\right)^{\frac{1}{2}}f(\eta),\ \theta(\eta)=\frac{T-T_\infty}{T_w-T_\infty} \tag{5a}$$

The radiative heat flux q_r is obtained by using the approximation of Rosseland for radiation as in [23–26],

$$q_r=-\frac{4\sigma^*}{3k^*}\frac{\partial T^4}{\partial y} \tag{5b}$$

T is implicit that the temperature varies within the flow, where the term T^4 is the linear function of the temperature. Therefore, on using Taylor series expansion to the term T^4 about T_∞ and on ignoring the higher order terms to get,

$$T^4\cong 4T_\infty^3T-3T_\infty^4$$

Then, Eq. (3) reduces to

$$u\frac{\partial T}{\partial x}+\mathrm{v}\frac{\partial T}{\partial y}=\frac{\kappa_{nf}}{(\rho c_p)_{nf}}\frac{\partial^2 T}{\partial y^2}-\frac{1}{(\rho c_p)_{nf}}\frac{16\sigma^* T_\infty^3}{3k^*}\frac{\partial^2 T}{\partial y^2}, \tag{5c}$$

On the implementation of similarity transformations (5a) and Eq. (5b) to governing Eqs. (2) and (3), we obtain,

$$\frac{C_2}{C_1}\frac{\partial^3 f}{\partial \eta^3}+f(\eta)\frac{\partial^2 f}{\partial \eta^2}-\left(\frac{\partial f}{\partial \eta}\right)^2+\beta\frac{C_2}{C_1}\left[\left(\frac{\partial^2 f}{\partial \eta^2}\right)^2-f(\eta)\frac{\partial^4 f}{\partial \eta^4}\right]-M\left(\frac{\partial f}{\partial \eta}-\lambda\right)\frac{C_3}{C_1}+\lambda^2=0, \tag{6}$$

$$(C_5+N_R)\frac{\partial^2\theta}{\partial \eta^2}+\Pr C_4 f\frac{\partial \theta}{\partial \eta}=0,\ \left(\text{for}\quad T_w(x)=T_w\right) \tag{7}$$

$$(C_5+N_R)\frac{\partial^2\theta}{\partial \eta^2}+\Pr C_4\left(f\frac{\partial \theta}{\partial \eta}-\frac{\partial f}{\partial \eta}\theta\right)=0,\ \left(for\ T_w(x)=T_w+bx\right) \tag{8}$$

also B.Cs are as follows:

$$\left.\begin{array}{lll} f(\eta)=V_c, & \frac{\partial f}{\partial \eta}=d+L_1\frac{\partial^2 f}{\partial \eta^2}, & \theta(\eta)=1 \text{ at } \eta=0 \\ \frac{\partial f}{\partial \eta}=\lambda, & \frac{\partial^2 f}{\partial \eta^2}=0, & \theta(\eta)=0 \text{ as } \eta\to\infty \end{array}\right\} \tag{9}$$

here, $\beta=\Gamma_2 c$ is Deborah number, $\lambda=\frac{a}{c}$ is stagnation/strength parameter, $M=\frac{\sigma_f B_0^2}{\rho_f c}$ is magnetic parameter, $C_1=\frac{\rho_{nf}}{\rho_f}$ and $C_2=\frac{\mu_{nf}}{\mu_f}$, $C_3=\frac{\sigma_{nf}}{\sigma_f}$, $C_4=\frac{(\rho c_P)_{nf}}{(\rho c_P)_f}$, $C_5=\frac{\kappa_{nf}}{\kappa_f}$. $P_r=\frac{\nu_f}{\alpha_f}$ is Prandtl number. V_c is mass transpiration parameter, for suction case $V_c>0$ and for injection case $V_c<0$, d is stretching/shrinking parameter, where $d>0$ for stretching and $d<0$ for shrinking, respectively. $L_1=A\left(\frac{c(1+\Gamma_1)}{\nu_f}\right)^{\frac{1}{2}}$ is first order slip. And nanofluid quantities are given by,

Here, φ is solid volume fraction of nanofluid. The physical quantities of interest, the skin friction coefficient and local Nusselt number, respectively, given by,

$$C_{\mathrm{f}} = \frac{v_f}{a^2x^2}\left(\frac{\partial u}{\partial y}\right)_{\mathrm{y}=0} = \frac{c}{a^2x}\left(cv_{\mathrm{f}}\left(1+\Gamma_1\right)\right)^{\frac{1}{2}}\left(\frac{\partial^2 f}{\partial \eta^2}\right)_{\eta=0},$$

$$Nu_{\mathrm{x}} = -x\left(\frac{c\left(1+\Gamma_1\right)}{v_{\mathrm{f}}}\right)^{\frac{1}{2}}\left(\frac{\partial \theta}{\partial \eta}\right)_{\eta=0} \tag{10}$$

Additionally the skin friction and Nusselt number can be determined from $-\left(\frac{\partial^2 f}{\partial \eta^2}\right)_{\eta=0}$ and $-\left(\frac{\partial \theta}{\partial \eta}\right)_{\eta=0}$

Analysis of momentum equation

The present work is related to classical Crane's [10] solution for the simple flow, that is for $\lambda = S = L_1 = 0$ and $d = 1$. For the general case, the solution form of momentum equation is as below and to get the physical solution there is an additional constraint as $\delta > 0$,

$$f(\eta) = V_{\mathrm{c}} + \lambda\eta + \frac{d-\lambda}{\delta\left(1+L_1\delta\right)}\left[1-\exp(-\delta\eta)\right] \tag{11}$$

Applying of Eq. (11) into Eq. (6) gives, C_1, C_2, C_3, C_4, C_5

$$\begin{aligned}(d-\lambda)\Bigg\{&\left(1+L_1\delta\right)\left[-\frac{C_3}{C_1}M+\delta\left(\frac{C_2}{C_1}\delta - V_{\mathrm{c}} + \frac{C_2}{C_1}\beta S\delta^2\right)\right]\\&+d\left(-1+\frac{C_2}{C_1}\beta\delta^2\right)-\lambda-2\lambda L_1\delta-\frac{C_2}{C_1}\beta\lambda\delta^2\\&+\eta\lambda\delta\left(1+L_1\delta\right)\left(-1+\frac{C_2}{C_1}\beta\delta^2\right)\Bigg\}=0\end{aligned} \tag{12}$$

For the special case $\lambda = 0$, Eq. (12) got the form as follows:

$$\begin{aligned}&d\left(-1+\frac{C_2}{C_1}\beta\delta^2\right)\left(1+L_1\delta\right)\\&+\left[-\frac{C_3}{C_1}M+\delta\left(\frac{C_2}{C_1}\delta - V_{\mathrm{c}} + \frac{C_2}{C_1}\beta S\delta^2\right)\right]=0\end{aligned} \tag{13}$$

Analysis of heat transfer

These momentum and temperature solutions got match with the examined work of Turkyilmazoglu [3, 6]. In the case of linear wall concentration, Eqs. (8) and (11) can lead us to obtain an additional solution by taking the assumption,

$$\theta(\eta) = \exp(-\delta\eta) \tag{14}$$

Applying Eq. (11) and (14) in Eq. (8) will imply,

$$C_4\,\mathrm{Pr}\,d + \left(1+L_1\delta\right)\delta\left[C_4V_c\,\mathrm{Pr} - \left(C_5+N_R\right)\delta\right] = 0, \tag{15}$$

Equation (13) and (15) gives the relations,

$$\delta = \sqrt{\frac{\left(C_5+N_{\mathrm{R}}\right)-\mathrm{Pr}\,\frac{C_4C_2}{C_1} \pm \sqrt{\left(\left(C_5+N_{\mathrm{R}}\right)-\mathrm{Pr}\,\frac{C_4C_2}{C_1}\right)^2+4\mathrm{Pr}\beta\frac{C_2C_3C_4}{C_1^2}\left(C_5+N_{\mathrm{R}}\right)M}}{2\beta\frac{C_2}{C_1}\left(C_5+N_{\mathrm{R}}\right)}}, \tag{16}$$

and

$$S = -\frac{d}{\delta\left(1+L_1\delta\right)} + \frac{\delta\left(C_5+N_R\right)}{C_4\,\mathrm{Pr}} \tag{17}$$

Here, δ and S is influenced by all used physical parameters.

And clearly for the above studied special case $\lambda = 0$, the velocity and concentration fields becomes,

$$f(\eta) = V_{\mathrm{c}} + \frac{d}{\delta\left(1+L_1\delta\right)}\left[1-\exp(-\delta\eta)\right], \tag{18}$$

and

$$\phi(\eta) = \exp(-\delta\eta) \tag{19}$$

Here, $\delta > 0$ and S are given by Eqs. (16) and (17). For this case, skin friction and Sherwood numbers becomes,

$$-\left(\frac{\partial^2 f}{\partial \eta^2}\right)_{\eta=0} = \frac{\delta d}{1+L_1\delta} \quad \text{and} \quad -\left(\frac{\partial \phi}{\partial \eta}\right)_{\eta=0} = \delta \tag{20}$$

The Jeffrey fluid will change to following f in case of $\lambda = d = 1$.

$$f(\eta) = V_{\mathrm{c}} + \eta, \tag{21}$$

Temperature profile is given by,

$$\theta(\eta) = \frac{\mathrm{Erfc}\left[\sqrt{\frac{\mathrm{Pr}\,C_4}{2(C_5+N_{\mathrm{R}})}}\left(V_{\mathrm{c}}+\eta\right)\right]}{\mathrm{Erfc}\left[\sqrt{\frac{\mathrm{Pr}\,C_4}{2(C_5+N_{\mathrm{R}})}}\,V_{\mathrm{c}}\right]}, \tag{22}$$

The function *Erfc* denotes the complementary error function. From Eq. (22) the Nusselt number will be obtained as follows:

$$-\theta_\eta(0) = \frac{-\sqrt{\frac{2\,\mathrm{Pr}\,C_4}{\pi(C_5+N_{\mathrm{R}})}}\mathrm{Exp}\left[-\frac{Pr}{(C_5+N_{\mathrm{R}})}\right]}{\mathrm{Erfc}\left[\sqrt{\frac{\mathrm{Pr}\,C_4}{2(C_5+N_{\mathrm{R}})}}\,V_{\mathrm{c}}\right]}. \tag{23}$$

Result and discussion

The current work examine the MHD slip flow and heat transfer of Jeffrey fluid due to a stretching/shrinking surface with CNTs considering the effects of thermal radiation and

Table 1 Thermophysical properties of CNTs [22]

Properties	Carbon nanotubes
Density	$\rho_{nf} = (1-\varphi)\rho_f + \varphi\rho_{CNT}$
Heat capacity	$(\rho c_p)_{nf} = (1-\varphi)(\rho c_p)_f + \varphi(\rho c_p)_{CNT}$
Dynamic viscosity	$\mu_{nf} = \frac{\mu_f}{(1-\varphi_1)^{2.5}}$
Thermal conductivity	$\frac{\kappa_{nf}}{\kappa_f} = \frac{1-\varphi+2\varphi\frac{\kappa_{CNT}}{\kappa_{CNT}-\kappa_f}\log\frac{\kappa_{CNT}+\kappa_f}{2\kappa_f}}{1-\varphi+2\varphi\frac{\kappa_f}{\kappa_{CNT}-\kappa_f}\log\frac{\kappa_{CNT}+\kappa_f}{2\kappa_f}}$
Electrical conductivity	$\frac{\sigma_{nf}}{\sigma_f} = 1 + \frac{3\varphi\left(\frac{\sigma_{CNT}}{\sigma_f}-1\right)}{\frac{\sigma_{CNT}}{\sigma_f}-2-\left(\frac{\sigma_{CNT}}{\sigma_f}-1\right)\varphi}$

Navier's slip. Further consider the effects of nanofluid by adding CNTs. This leads to offer higher thermal conductivity than base fluid and considered nanofluid is formed by suspending two types of CNTs, i.e. SWCNTs and MWCNTs in the base fluid water. The structure of the problem is equation of momentum and temperature which are then converted into a set of ODE's to imitate the MHD flow of carbon nanotubes. Magnetic parameter (M), radiation parameter (N_R), and Navier slip (L_1) effect significantly on the structure of solution of the problem. And investigate the important physical parameters Nusselt number and skin friction. In all plots, black curves denote SWCNTs and red curves denote MWCNTs. Moreover, the thermophysical properties are mentioned in Table 1. The present research is good agreement with already existing literature [19].

Figures 2 and 3, respectively, demonstrate the transverse and axial velocity for different entities of magnetic parameter M. In Fig. 2, Pr is fixed at 6.2 for base fluid water for SWCNTs and MWCNTS. It can be seen that velocity

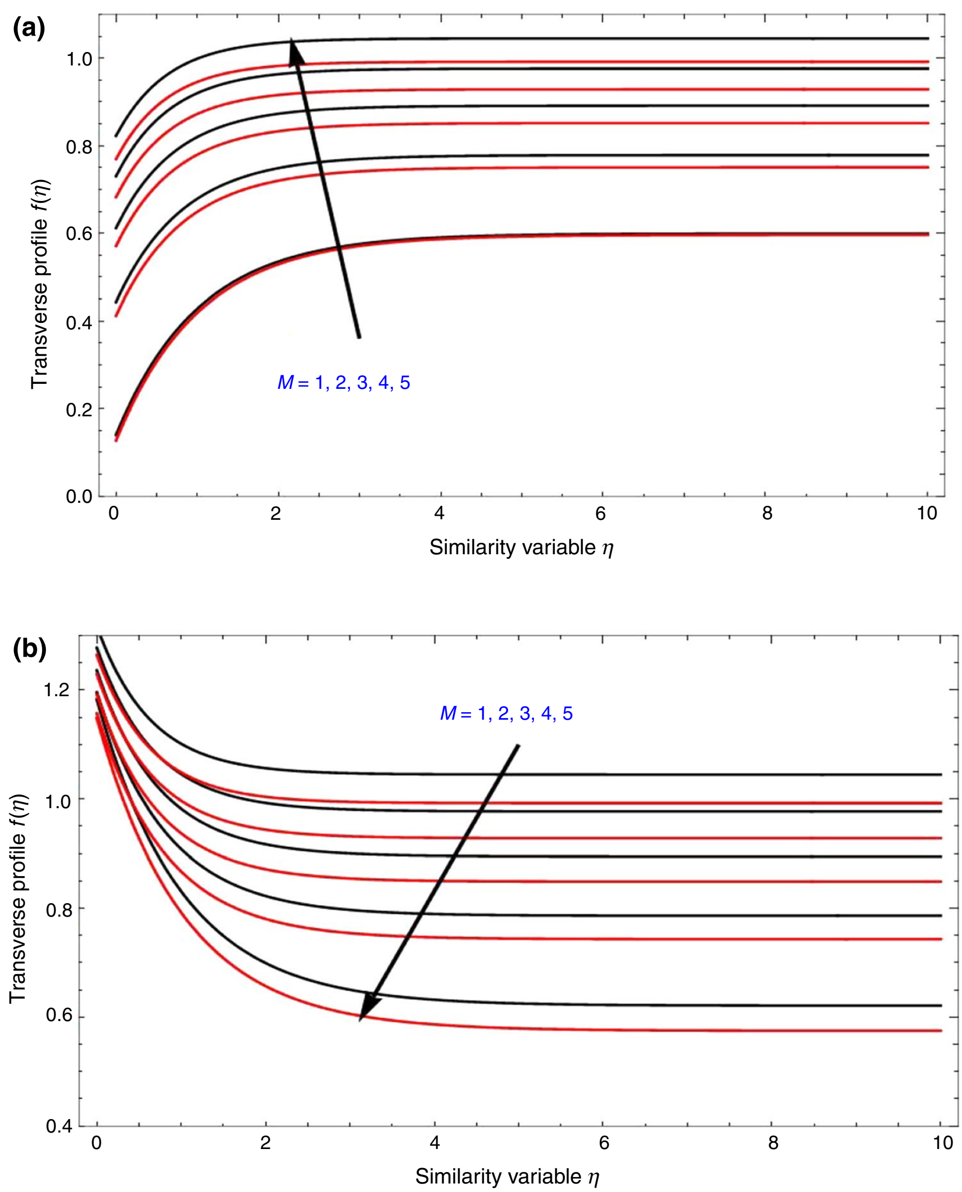

Fig. 2 The transverse velocity profile $f(\eta)$ for various values of magnetic parameter M due to **a** stretching sheet and **b** shrinking sheet

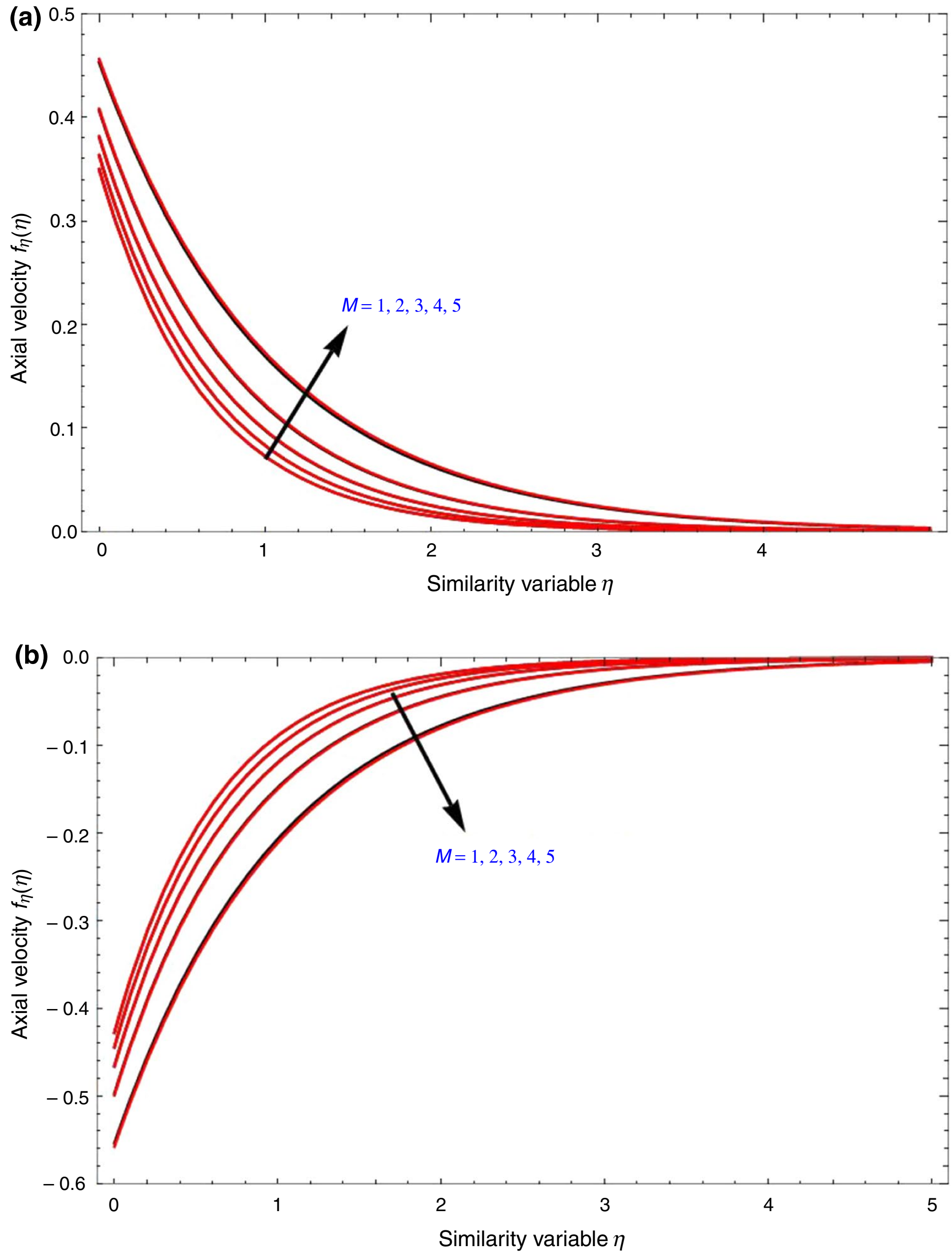

Fig. 3 The axial velocity profile $f_\eta(\eta)$for various values of magnetic parameter M due to **a** stretching sheet and **b** shrinking sheet

profiles increases with raise in M for stretching boundary. Similarly, we can also notice that velocity profiles decreases with raise in M for shrinking boundary. Transverse velocity improves for water and kerosene oil nanofluid for SWCNT than MWCNT. If MWCNT nanofluids have higher effective velocities than the SWCNT-deferred nanofluids, and this might assist in industrial applications and medical benefits. But axial velocity has no much difference for SWCNTs and MWCNTs. The impact of Radiation parameter N_R on axial velocity $f_\eta(\eta)$ is examined in Fig. 4. The axial velocity profile for SWCNTs and MWCNTs using base liquid water indicates a reduction for the behaviour of N_R. The consequence of increase of N_R on axial velocity will be, increased $f_\eta(\eta)$

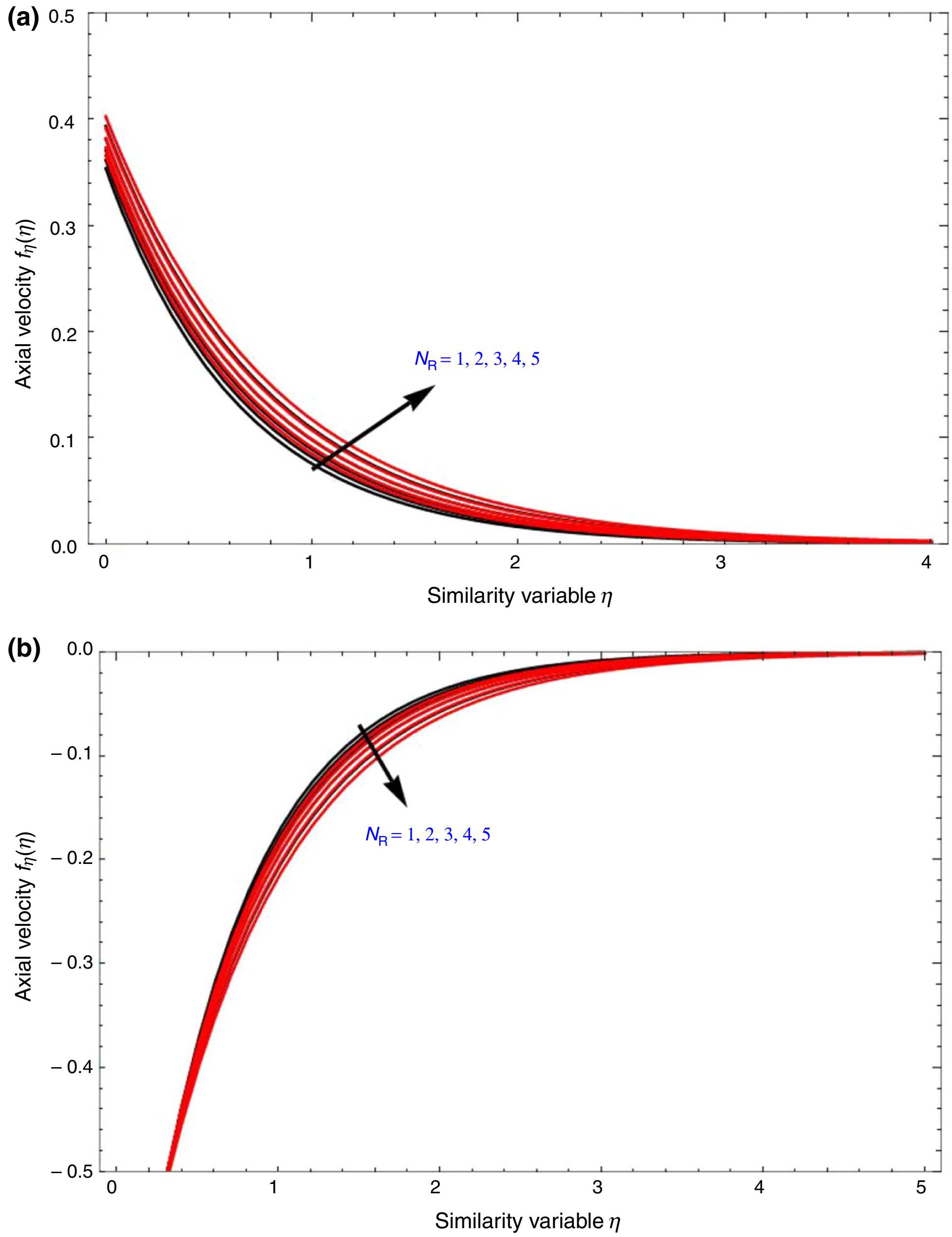

Fig. 4 The transverse velocity profile $\mathrm{Pr} f_\eta(\eta)$ for various values of radiation parameter N_R due to **a** stretching sheet and **b** shrinking sheet

for stretching boundary and decreased $f_\eta(\eta)$ for shrinking boundary.

Figure 5a depicts the skin friction C_f verses Prandtl number Pr for different values of *M*. The skin friction is more for SWCNTs than for MWCNTs and is negative. With the increase in *M*, the skin friction will decrease. In the similar way, the variation of skin friction C_f verses *M* for different values of *Pr* is as shown in Fig. 5b. With the increase in Pr, the skin friction will decrease. C_f will increase with dense of volume fraction and decreases with Navier slip because of an increase in CNT density with solid volume fraction.

Figure 6 portrays the effect of *M* and V_C on temperature profile $\theta(\eta)$. From Fig. 6a, the observations can be made

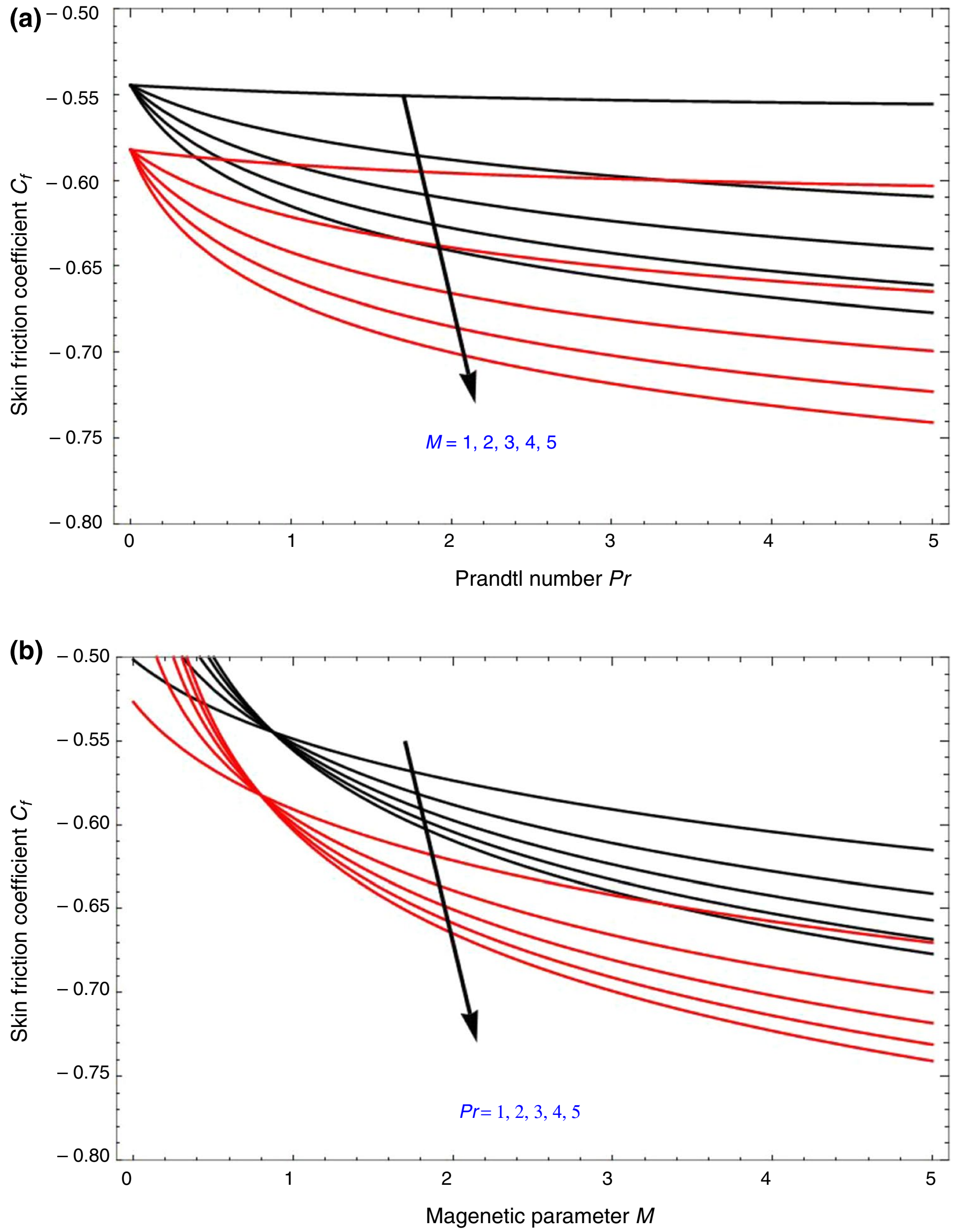

Fig. 5 The Skin friction coefficient C_f **a** versus Pr for different values of M and **b** C_f **a** versus M for different values of Pr due to stretching sheet

are, raise in M for both SWCNT and MWCNTs will result in decrease of thermal boundary layer thickness. For lower value of M, there is a temperature difference for SWCNTs and MWCNTs, further can be seen that on increasing M, the difference is negligible.

Figure 6b represents the impact of V_C on temperature profile $\theta(\eta)$. In both the SWCNT and MWCNT cases, temperature decreases with increase in V_C. This is because of the way that fluid has a lower thermal conductivity for a comprehensive mass transpiration, which lessens

Fig. 6 The temperature profile $\theta(\eta)$ for various values of radiation parameter N_R due to **a** stretching sheet and **b** shrinking sheet

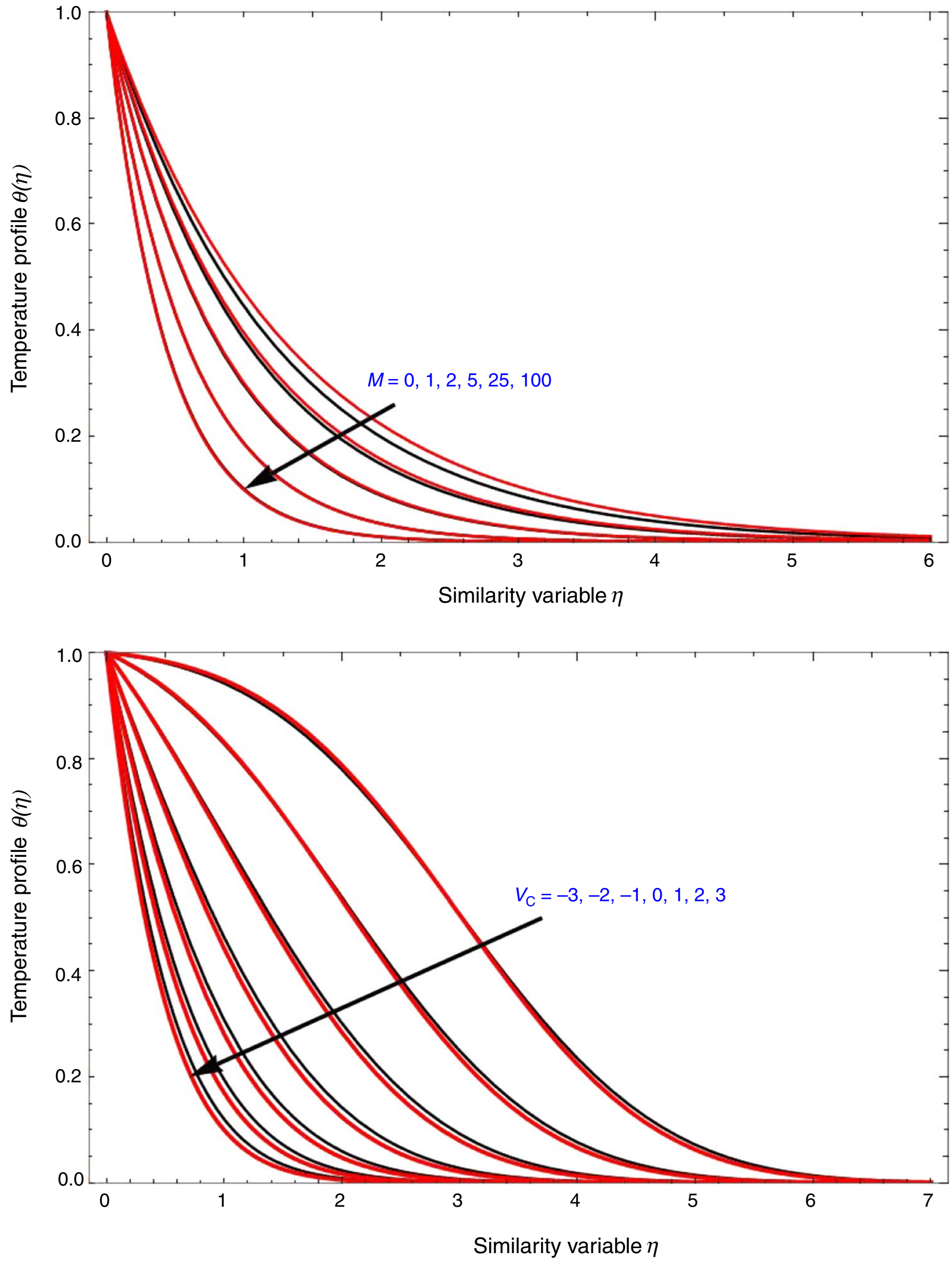

conduction and the thickness of the thermal boundary layer, lowering the temperature.

Figure 7 depicts the effect of Pr on Nusselt number which plot versus mass transpiration V_C. It can be observed the improvement in the rate of heat transfer as V_C increases. And also Nusselt number will be more for more value of Pr and the Nusselt number for SWCNTs is less than that for MWCNTs.

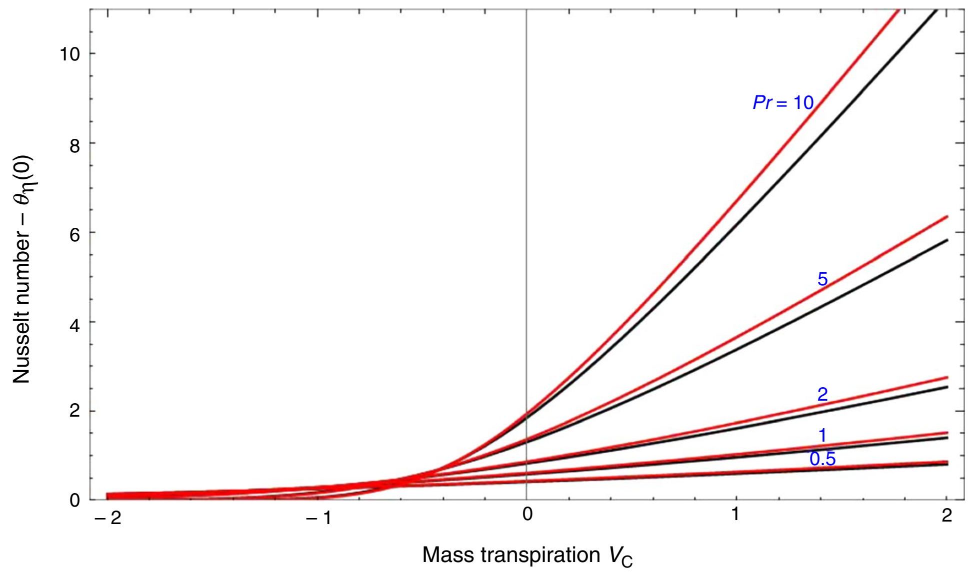

Fig. 7 The Nusselt number $-\theta_\eta(0)$ verses mass transpiration V_C for various values of Pr due to stretching sheet

Conclusions

The examination of MHD slip flow and heat transfer of Jeffrey fluid due to a stretching/shrinking surface with CNTs considering the effects of thermal radiation and Navier's slip will result in some observations. Further consider the effects of nanofluid by adding CNTs to offer higher thermal conductivity than base fluid. The governing partial differential equations for momentum and energy are transformed into ordinary differential equations using a similarity transformation. These equations are solved analytically. MWCNT suspended nanofluids have evolved faster velocities than SWCNT suspended nanofluids, indicating that they may be beneficial in a few applications. Primary research has shown that MWCNT nanoparticles can reach the tumour faster than SWCNT nanoparticles in the treatment of disorder. Magnetic parameter (M), radiation parameter $\left(N_R\right)$, and Navier slip $\left(L_1\right)$ effect significantly on the structure of solution of the problem is discussed. And investigate the important physical parameters Nusselt number and skin friction.

- Velocity profiles increases with increase in magnetic field for stretching boundary and decreases with increase in magnetic field for shrinking boundary.
- The axial velocity profile for SWCNTs and MWCNTs using base liquid water indicates a reduction for the behaviour of radiation parameter.
- Increase of radiation parameter on axial velocity will results in, axial velocity increased for stretching boundary and decreased for shrinking boundary.
- The skin friction is more for SWCNTs than for MWCNTs and is negative.
- Increase of magnetic field or Prandtl number will decrease the skin friction.
- In both the SWCNT and MWCNT cases, temperature decreases with increase in mass transpiration.
- The rate of heat transfer will improve as mass transpiration increases. And also Nusselt number will be more for more value of Prandtl number.
- Nusselt number for SWCNTs is less than that for MWCNTs

A number of previous studies serve as the limiting example for this investigation.

(a) $\lim\limits_{\substack{M\to 0,\\ \phi\to 0,\\ q_r\to 0,}}$ {Results of present works}→{ Results of Turkyilmazoglu [19]}.

Further extensions of the current work can be implemented incorporating new physical mechanisms, such as an external Newtonian/non-Newtonian fluid rheology with various parameter.

References

1. Ebaid A, Sharif MA. Application of Laplace trans-form for the exact effect of a magnetic field on heat transfer of carbon nanotubes-suspended nanofluids. Z Naturforsch. 2015;70:471–5.
2. Sarpakaya T. Flow of non-Newtonian fluids in a magnetic field. AIChEJ. 1961;7:324–8.
3. Mahabaleshwar US. External regulation of convection in a weak electrically conducting non-Newtonian liquid with g-jitter. J Magn Magn Mater. 2008;320:999–1009.
4. Mahabaleshwar US. Combined effect of temperature and gravity modulations on the onset of magneto-convection in weak electrically conducting micropolar liquids. Int J Eng Sci. 2007;45:525–40.

5. Mahabaleshwar US, Nagaraju KR, Vinay Kumar PN, Nadagouda MN, Bennacer R, Sheremet MA. Effects of Dufour and Sort mechanisms on MHD mixed convective-radiative non-Newtonian liquid flow and heat transfer over a porous sheet. J Ther Sci Eng Prog. 2020;16: 100459.
6. Tiwari AK, Raza F, Akhtar J. Mathematical model for Marangoni Convection MHD flow of Carbon nanotubes through a porous medium. IAETSD J Adv Res Appl Sci. 2017;4:216–22.
7. Crane L. Flow past a stretching plate. Zeitschift fur Ange-wand-teMath Phys. 1970;21:645–7.
8. Sakiadis BC. Boundary layer behavior on continuous solid surface. AIchE J. 1961;7:26.
9. Hayat T, Hussain Z, Alsaedi A, Asghar S. Carbon nanotubes effects in the stagnation point flow towards a nonlinear stretching sheet with variable thickness. Adv Powder Technol. 2016;27:1677–88.
10. Hamad MAA. Analytical solution of natural convection flow of a nanofluid over a linearly stretching sheet in the presence of magnetic field. Int Commun Heat Mass Transf. 2011;38:487–92.
11. Fang T, Zhang J. Closed-form exact solutions of MHD viscous flow over a shrinking sheet. Commun Nonlinear Sci Numer Simul. 2009;14:2853–7.
12. Vinay Kumar PN, Mahabaleshwar US, Nagaraju KR, Mousavi Nezhad M, Daneshkhah A. Mass transpiration in magnetohydrodynamic boundary layer flow over a superlinear stretching sheet embedded in porous medium with slip. J Porous Media. 2019;22:1015–25.
13. Sneha KN, Mahabaleshwar US, Bhattacharyya S. Consequences of mass transpiration and thermal radiation on Jeffery fluid with nanofluid. Num Heat Transf Part A Appl. 2023;1:1–13.
14. Turkyilmazoglu M. Multiple analytic solutions of heat and mass transfer of magnetohydrodynamic slip flow for two types of viscoelastic fluids over a stretching surface. J Heat Transf. 2012;134:071701–11.
15. Reddy SRR, Reddy PBA, Chamkha AJ. MHD flow analysis with water-based CNT nanofluid over a non-linear inclined stretching/shrinking sheet considering heat generation. Chem Eng Trans. 2018;71:1003–8.
16. Norzawary NHA, Bachok N, Ali FMd. Stagnation point flow over a stretching/shrinking sheet in some Carbon nanotubes with suction/injection effects. CFD Lett. 2020;12:106–14.
17. Mahabaleshwar US, Sneha KN, Huang H-N. An effect of MHD and radiation on CNTS-Water based nanofluid due to a stretching sheet in a Newtonian fluid. Case Stud Therm Eng. 2021;28:101462.
18. Mahabaleshwar US, Anusha T, Hatami M. The MHD Newtonian hybrid nanofluid flow and mass transfer analysis due to superlinear stretching sheet embedded in porous medium. ScientificReports. 2021. https://doi.org/10.1038/s41598-021-01902-2.
19. Turkyilmazoglu M, Pop I. Exact analytical solutions for the flow and heat transfer near the stagnation point on a stretching/shrinking sheet in a Jeffrey fluid. Int J Heat Mass Transf. 2013;57:82–8.
20. Saif RS, Muhammad T, Sadia H, Ellahi R. Hydromagnetic flow of Jeffrey nanofluid due to a curved stretching surface. Physica A. 2020;551: 124060.
21. Rao ME, Sreenadh S. MHD Boundary Layer Flow of Jeffrey Fluid over a Stretching/Shrinking sheet through porous Medium. Global J Pure Appl Math. 2017;13:3985–4001.
22. Maranna T, Sneha KN, Mahabaleshwar US, Sarris IE, Karakasidis TE. An effect of radiation and MHD Newtonian fluid flow over a stretching/shrinking sheet with CNTs and mass transpiration. Appl Sci. 2022;12:5466.
23. Rosseland LA. Astrophysik and atomtheoretische Grundlagen. Berlin: Springer-Verlag; 1931.
24. Cortell R. Radiation effects for the Blasius and Sakiadis flows with a convective surface boundary condition. Appl Math Comput. 2008;206:832–40.
25. Mahabaleshwar US, Nagaraju KR, Vinay Kumar PN, Nadagouda MN, Bennacer R, Baleanu D. An MHD viscous liquid stagnation point flow and heat transfer with thermal radiation and transpiration. Therm Sci Eng Prog. 2019;16:100379.
26. Maranna T, Sachhin SM, Mahabaleshwar US, Hatami M. Impact of Navier's slip and MHD on laminar boundary layer flow with heat transfer for non-Newtonian nanofluid over a porous media. Sci Rep. 2023;13:12634.